Issues in Structural Health Monitoring Employing Smart Sensors

T. Nagayama[1], S. H. Sim[1], Y. Miyamori[2], and B. F. Spencer, Jr.[3]

ABSTRACT

Smart sensors densely distributed over structures can provide rich information for structural monitoring using their onboard wireless communication and computational capabilities. However, issues such as time synchronization error, data loss, and dealing with large amounts of harvested data have limited the implementation of full-fledged systems. Limited network resources (e.g., battery power, storage space, bandwidth, etc.) make these issues quite challenging. This paper first investigates the effects of time synchronization error and data loss, aiming to clarify requirements on synchronization accuracy and communication reliability in SHM applications. Coordinated computing is then examined as a way to manage large amounts of data.

Keywords: coordinated computing; data compression; distributed computing strategy; smart sensors; time synchronization; data loss; data aggregation

1. INTRODUCTION

The investment of the United States in civil infrastructure is estimated to be $20 trillion. Annual costs amount to between 8-15% of the GDP for most industrialized countries

[1] Doctoral Candidate, Dept. of Civil and Environmental Engineering, University of Illinois at Urbana-Champaign, Urbana, IL 61801, USA
[2] Assistant Professor, Kitami Institute of Technology, Hokkaido 090-8507, Japan
[3] Nathan M. and Anne M. Newmark Endowed Chair of Civil Engineering, University of Illinois at Urbana-Champaign, Urbana, IL 61801, USA

(U.S. Census 2004; Jensen 2003). This investment is likely to increase; for example, the U.S. Department of Transportation (2003) has reported that the capital investment to preserve highways and bridges increased 45.7% from $23.2 billion in 1997 to $33.6 billion in 2000. Indeed, much attention has been focused in recent years on the declining state of the aging infrastructure in the U.S. These concerns apply not only to civil engineering structures, such as the nation's bridges, highways, and buildings, but also to other types of structures, such as the aging fleet of aircraft currently in use by domestic and foreign airlines. The ability to continuously monitor the integrity of civil infrastructures in real-time offers the opportunity to reduce maintenance and inspection costs, while providing for increased safety to the public. Furthermore, after natural disasters, it is imperative that emergency facilities and evacuation routes, including bridges and highways, be assessed for safety. Addressing all of these issues is the objective of structural health monitoring (SHM).

To efficaciously investigate damage, a dense array of sensors is required for large civil engineering structures. (Spencer et al. 2004, Gao 2005). Dense measurement is expected to provide detailed information on civil infrastructure, which typically consists of a large number of components and has many degrees of freedom. Monitoring the Tsing Ma Bridge and Kap Shui Mun Bridge in Hong Kong, which uses 326 channels of sensors and produces about 65 MB of data every hour, is an attempt toward in-depth monitoring (Wong 2004). Expensive installation of traditional monitoring systems, however, has limited significantly wider spread implementation (Lynch and Loh 2006, Farrar 2001, and Celebi 2002). Smart sensors with wireless communication capability are reported to reduce installation effort to a great extent (Lynch et al. 2005) and help to realize a dense array of sensors.

Though networks of densely deployed smart sensors have the potential to improve SHM dramatically, limited resources on smart sensors preclude direct application of traditional monitoring strategies on smart sensor networks. Time synchronization among smart sensors is not as accurate as for a wired system. Data transfer between sensor nodes is less reliable than in a wired system due to data loss. Transferring all data to a central station using wireless communication is not practical or scalable, especially in a system employing a dense array of smart sensors. Moreover, battery power often imposes practical limits on these functionalities. Although many researchers have reported difficulties in data transfer rates and reliability, as well as time synchronization (Casciati et al. 2003, Elson et al. 2002, Kottapalli et al. 2003, Mechitov et al 2003, Mosalam 2003, Kurata et al. 2004 Wang et al. 2005), the effects on SHM and ways to address these issues have not been studied in depth. Careful investigation can provide insight into how to accommodate these difficulties from a SHM perspective.

This paper studies issues associated with SHM applications employing smart sensor networks. Several issues critical to realizing a SHM system using smart sensors are first described. Among them, the effects of time synchronization error and data loss are investigated from a SHM perspective. Coordinated computing is examined as a way to manage large amounts of data. Numerical simulation and experimental testing validate the derivation and proposals.

2. SHM EMPLOYING SMART SENSORS

Smart sensors with computational and communication capabilities have been employed for SHM research. Some of the first efforts in developing smart sensors for application to civil engineering structures were presented by Straser and Kiremidjian (1996, 1998) and Kiremidjian et al. (1997). Since these initial efforts, numerous researchers have developed smart sensing platforms (Lynch and Loh 2005). With respect to functionality, most of early attempts simply replaced wired communication with RF links. Together with introduction of battery power at the sensor nodes, RF communication eliminated the need for cabling. Such measurement systems with wireless communication links, however, encounter many difficulties, e.g., slow and unreliable communication, inaccurate time synchronization among sensor nodes, insufficient sensing capabilities, and limited power. While smart sensor's computational capability potentially offers new opportunities for SHM, these issues need to be carefully examined before a functional SHM system can be realized.

Among the issues is lossy RF communication, which can severely impair a SHM system. Structural analysis generally assumes data acquired at specified time interval is available with certain accuracy. While measurement noise and quantization errors are usually considered primary sources of errors, data loss has not been considered as an error source in traditional SHM systems because all the data is reliably transferred in a wired system. This assumption does not apply to wireless systems; many researchers have reported data loss during wireless communication (Casciati et al. 2003, Mosalam 2003, Kurata et al. 2004). Mechitov et al. (2003) addressed this communication reliability problem by utilizing acknowledgement messages. However,

reliable communication is stated to be slow due to associated header information and acknowledgement messages, using more resources of a system. Studies of the data loss effect on structural analysis are needed to assess the use of more expensive reliable communication versus simple lossy communication.

Time synchronization error in a smart sensor network is another source of inaccuracy in SHM applications. Each sensor node has its own clock. By communicating with surrounding nodes, smart sensors can assess relative difference among their local clocks. Well-known algorithms include Reference Broadcast Synchronization (Elson et al. 2002), Flooding Time Synchronization Protocol (Maroti et al. 2004), and Timing-sync Protocol for Sensor Networks (Ganeriwal et al. 2003). Time synchronization is, however, not as accurate as for a wired networked system. Also, the local clock of a smart sensor can have large drift in time and need to synchronize with each other repeatedly to maintain certain synchronization accuracy. Time synchronization error problems have been reported both in laboratory and in full-scale bridge monitoring applications using smart sensors (Lynch et al. 2005). Requirements on synchronization accuracy need to be investigated from a SHM perspective.

Data aggregation is especially problematic for SHM applications which typically require large amounts of data. For example, 2-byte data samples collected at 100 Hz generate 12 KB of data every minute. While the CC1000, one of RF chips adapted in several early smart sensor platforms, supports 38.4kbps data rate, the actual rate at which measurement data is transferred is much slower because of packet collision, packet headers, etc. Acknowledgement messages associated with reliable communication reduce data transfer speeds even more. A centralized data collection

system, which simply replaces the wired links of a traditional SHM system with RF links, therefore, cannot handle the massive amounts of data acquired concurrently at hundreds of sensor nodes (see Fig. 1).

Several researchers have attempted to address the data aggregation problem. Tiered networks (Govindan et al. 2005) help centrally collect a large amount of data using several powerful master nodes together with smart sensor end nodes, though the usage is limited to applications in which use of powerful master nodes is viable; cost to install master nodes and the number of required master nodes are factors in determining its practicality. Another approach to address this data aggregation problem is independent data processing as shown in Fig. 2. Each smart sensor independently measures and processes data, typically using same pattern recognition, without sharing information among the neighboring nodes (Sohn et al. 2002, Lynch et al. 2005, Nitta et al. 2005). Because only the processed data is sent back to the base station, communication requirements are relatively small. However, from a SHM perspective, this approach can not utilize available spatial information from neighboring nodes (e.g. mode shapes). The inability of this approach to incorporate spatial information limits its effectiveness in SHM applications. Data aggregation utilizing distributed computing (Gao 2005, Nagayama et al. 2006) has the potential to achieve effective SHM employing smart sensors. Application specific knowledge is utilized to efficiently aggregate information in a distributed and coordinated manner (see Figure 3). Though this concept has been proposed, only partial implementation of this concept has been reported so far (Nagayama et al 2006). Implementation of the concept is expected to demonstrate a way to address the data aggregation problem in SHM applications.

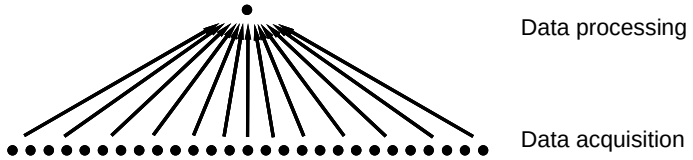

Fig. 1 Centralized data collection

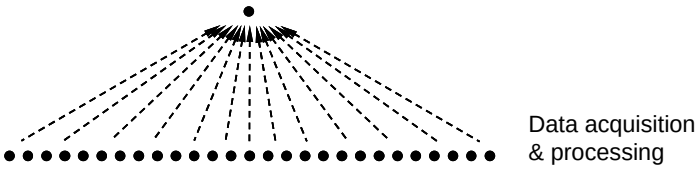

Fig. 2 Independent data processing

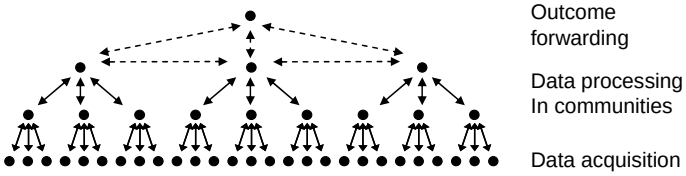

Fig. 3 Coordinated computing strategy

3. Effect of Time Synchronization Error on SHM

Time synchronization error in a smart sensor network can cause inaccuracy in SHM applications. Time synchronization is a middleware service common to smart sensor applications and has been widely investigated. Each smart sensor has its own local clock, which is not synchronized initially with other sensor nodes. By communicating with surrounding nodes, smart sensors can assess relative difference among their local clocks. For example, Mica2 motes employing TPSN are reported to synchronize with each other to an accuracy of 50μsec; different algorithms and hardware resources may result in different precision. Whereas time synchronization protocols have been intensively studied, requirements on synchronization from an application perspective are lacking. In many SHM applications, commonly used quantities include cross spectral density

(CSD), power spectral density (PSD), correlation function, and modal parameters. The effects of synchronization error on these estimates are discussed in this section.

3.1. Modeling of time synchronization error

Consider a signal from a smart sensor in local clock coordinate $\bar{x}(t)$ can be written using a signal in the reference clock, or the global clock $x(t)$ as

$$\bar{x}(t) = x\left((1+\alpha)t - t_j\right) \quad \text{Eq. (1)}$$

where t_j is the initial time synchronization error and α is the clock drift rate. In the frequency domain, this relationship is expressed as

$$\bar{X}(\omega) = \frac{1}{1+\alpha} e^{-i\omega\frac{t_j}{1+\alpha}} X\left(\frac{\omega}{1+\alpha}\right) \quad \text{Eq. (2)}$$

where $X(\omega)$ and $\bar{X}(\omega)$ are the Fourier transform of $x(t)$ and $\bar{x}(t)$, respectively. Clock drift is oftentimes small. In the following derivation α is assumed to be zero.

3.2. Impact of time synchronization error in input-output identification

Change in the estimation of modal parameters due to the poorly synchronized input and output can be identified by looking into the transfer function. If the *m*-th input and *n*-th output are shifted by t_m^{in} and t_n^{out}, respectively, the transfer function $\bar{H}_{nm}(\omega)$ between the shifted input and output is written as

$$\begin{aligned} \bar{H}_{nm}(\omega) &= \frac{\bar{Y}_n(\omega)}{\bar{F}_m(\omega)} = \frac{e^{-i\omega t_n^{out}} Y_n(\omega)}{e^{-i\omega t_m^{in}} F_m(\omega)} = e^{i\omega(t_m^{in} - t_n^{out})} H_{nm}(\omega) \\ &= e^{i\omega t_{nm}} H_{nm}(\omega) \end{aligned} \quad \text{Eq. (3)}$$

where $t_{nm} = t_m^{in} - t_n^{out}$. From Eq. (3), the magnitude of transfer function remains

unchanged while its phase is shifted by t_{nm}. When modal parameters are estimated from this transfer function, the natural frequency, damping ratio, and magnitude of the mode shape remain unchanged; only the phase of mode shapes is affected by the time synchronization error. The phase shift ϕ_k of the *k*-th mode is estimated as follows,

$$\phi_k = 2\pi f_k t_{nm} \qquad \text{Eq. (4)}$$

where f_k is the natural frequency of the *k*-th mode.

3.3. Impact of time synchronization error in output-only identification

The effect of time synchronization errors on modal parameters such as the natural frequency, damping ratio, and mode shape are examined for the case when only output measurement is available. When the excitation can be assumed to be broadband and the structural response stationary, the correlation function between the output measurements can be used to determine modal parameters by virtue of the Natural Excitation Technique (NExT) (James et al. 1992). Investigating the correlation function, change in modal parameters due to the time synchronization inaccuracy can be identified.

For completeness, NExT is briefly reviewed here. Consider the equation of motion in Eq. (5) under the assumption that the random responses are stationary.

$$M\ddot{x}(t) + C\dot{x}(t) + Kx(t) = f(t) \qquad \text{Eq. (5)}$$

where M, C, and K are the n x n mass, damping, and stiffness matrices, respectively; $x(t)$ is a n x 1 displacement vector; $f(t)$ is a m x 1 force vector; $\dot{x}(t)$ and $\ddot{x}(t)$ are the velocity and the acceleration vector. By multiplying displacement at reference sensor and taking expected value, Eq. (5) is transformed as follows.

$$ME\left[\ddot{x}(t+\tau)x_{ref}(t)\right]+CE\left[\dot{x}(t+\tau)x_{ref}(t)\right] \\ +KE\left[x(t+\tau)x_{ref}(t)\right]=E\left[f(t+\tau)x_{ref}(t)\right] \quad \text{Eq. (6)}$$

Because the input force and response at the reference sensor location are uncorrelated for $\tau \geq 0$, the right hand side is zero. The expectation between the two signals is the correlation function. Therefore, by denoting $E\left[x(t+\tau)y(t)\right]$ as the correlation function $R_{xy}(\tau)$, Eq. (6) is rewritten as

$$MR_{\ddot{x}x_{ref}}(\tau)+CR_{\dot{x}x_{ref}}(\tau)+KR_{xx_{ref}}(\tau)=0, \quad \tau>0. \quad \text{Eq. (7)}$$

When $\dot{A}(t)$ and $B(t)$ are weakly stationary processes, the following relation holds (Bendat and Piersol 2000).

$$R_{AB}(\tau)=\dot{R}_{AB}(\tau) \quad \text{Eq. (8)}$$

A similar relation holds for higher derivatives.

$$R_{A^{(m)}B}(\tau)=R_{AB}^{(m)}(\tau) \quad \text{Eq. (9)}$$

where the superscript, *m*, denotes the *m*-th derivative. Consequently, Eq. (7) can be rewritten as

$$M\ddot{R}_{xx_{ref}}(\tau)+C\dot{R}_{xx_{ref}}(\tau)+KR_{xx_{ref}}(\tau)=0, \quad \tau>0. \quad \text{Eq. (10)}$$

Thus, the correlation function for the stationary responses is shown to satisfy the equation of motion for free vibration. This fact can be directly used for modal analysis such as Eigensystem Realization Algorithm (ERA) (Juang and Pappa 1985).

Time synchronization errors enter into correlation function estimation. Consider a cross correlation function $R_{x_i x_{ref}}(\tau)$ between a response $x_i(t)$ at location *i*

and the reference signal $x_{ref}(t)$. The sensor node at location i has a time synchronization error of t_{x_i} relative to the reference node. The correlation function, $\overline{R}_{x_i x_{ref}}(\tau)$, under the synchronization error, can be written as

$$\overline{R}_{x_i x_{ref}}(t) = E\left[x_i(t - t_{x_i} + \tau)x_{ref}(t)\right] = R_{x_i x_{ref}}(t - t_{x_i}) \qquad \text{Eq. (11)}$$

If t_{x_i} is positive, the correlation function for the interval (0, t_{x_i}) does not have the same characteristics as the succeeding signal. In a structural analysis context, this portion has negative damping; therefore, the beginning portion of the signal needs to be removed. When t_{x_i} is unknown, a segment corresponding to the maximum possible time synchronization error, $t_{x_{\max}}$, is truncated from the correlation function.

The correlation functions, each having independent time synchronization errors, do not satisfy the equation of motion, Eq. (10). The correlation functions after the truncation, however, can be decomposed into modal components as follows

$$\begin{aligned}
&R_{x'x_{ref}'}(\tau) = \Phi' \Lambda A \\
&\Phi' = \left[\varphi_1' \quad \varphi_2' \quad \cdots \quad \varphi_{2n}'\right] \\
&\quad = \begin{bmatrix} \phi_{11}\exp\left(-\lambda_1 t_{x_1}\right) & \phi_{21}\exp\left(-\lambda_2 t_{x_1}\right) & \cdots & \phi_{2n1}\exp\left(-\lambda_{2n} t_{x_1}\right) \\ \phi_{12}\exp\left(-\lambda_1 t_{x_2}\right) & \phi_{22}\exp\left(-\lambda_2 t_{x_2}\right) & \cdots & \phi_{2n2}\exp\left(-\lambda_{2n} t_{x_2}\right) \\ \vdots & \vdots & \ddots & \vdots \\ \phi_{1m}\exp\left(-\lambda_1 t_{x_m}\right) & \phi_{2m}\exp\left(-\lambda_2 t_{x_m}\right) & \cdots & \phi_{2nm}\exp\left(-\lambda_{2n} t_{x_m}\right) \end{bmatrix} \\
&\Lambda = diag\left(\left[\exp(\lambda_1\tau) \quad \exp(\lambda_2\tau) \quad \cdots \quad \exp(\lambda_{2n}\tau)\right]\right) \\
&\lambda_i = -h_i\omega_i + j\omega_i\sqrt{1-h_i^2} \\
&A = diag\left(\left[a_1 \quad a_2 \quad \cdots \quad a_{2n}\right]\right)
\end{aligned} \qquad \text{Eq. (12)}$$

where $R_{x'x_{ref}'}(\tau)$ is the correlation function matrix on the interval $\left(t_{x_{\max}}, \infty\right)$, ϕ_{ij} is j-th

element of *i*-th mode shape, h_i and ω_i are *i*-th modal damping ratio and modal natural frequency, respectively, and a_i is a factor accounting for the relative contribution of the *i*-th mode in the correlation function matrix. Modal analysis techniques such as ERA can be used to identify these modal parameters. As Eq. (12) shows, the natural frequencies and damping ratios remain the same. The observed mode shapes Φ' are different from the original mode shapes; changes in mode shape amplitude are negligible due to small h_i and t_{x_i}, while phase shift can be meaningful. Mode shape phases can indicate structural damage and are important modal characteristics from a SHM perspective (Nagayama et al. 2005). Time synchronization error of 1ms results in about 3.6 degree phase delay of a mode at 10 Hz, while the same time synchronization error causes 36 degree phase delay at 100 Hz. The phase delay tolerance depends on the applications. When change in phase is investigated as in Nagayama et al. (2005), even 3.6 degree phase delay is considered to obscure the detail. The requirements on the time synchronization for modal analysis need to be assessed mainly from the viewpoint of mode shape phases.

3.4. Numerical simulation in 2 DOF model

To confirm the analytical investigation in the previous section, a numerical simulation is conducted using the 2 DOF model shown in Fig. 4. In this example, the natural frequencies and damping ratios of the model are listed in Table 2. Two independent band limited white noise inputs are imposed on the nodes, and accelerations of the lumped masses are simulated with the sampling time of 1 msec. 50 sample time histories are obtained for different input excitations and each time history is 81.91 seconds long. Several cases of time synchronization errors ($\Delta\tau$=1, 3, 5, 10, 25, 50, 100

msec) are considered for the simulated acceleration data of the 2nd nodal point.

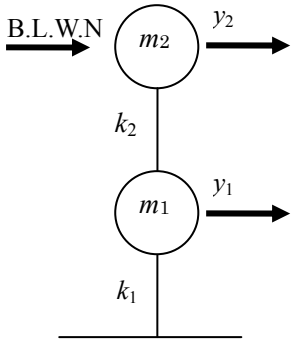

Fig. 4 Analytical model

Table 1 2DOF model

Mass (kg)	m_1	1
	m_2	2
Stiffness (N/m)	k_1	200
	k_2	400

Table 2 Natural frequency and damping ratio

Mode	Natural frequency (Hz)	Damping ratio
1st	1.261	0.01
2nd	4.018	0.01

Input-output and output-only identification methods are applied to estimate the mode shapes of the system. The transfer functions calculated from the unsynchronized input force and output accelerations are used to obtain the operational mode shapes. Eq. (3) is used to get the transfer functions analytically for comparison. In addition, NExT/ERA is used to estimate the mode shapes by using only output accelerations. Since the natural frequency and damping ratio are invariant under the time synchronization error, only changes in the mode shapes are considered.

The calculated mode shapes are shown in Fig. 5 and Fig. 6 with respect to the time synchronization errors. The left figures represent the ratio between the mode shape amplitudes of the two nodes, and right figures are the phase delay between the two

nodes. As expected, phase delay significantly changes as the time synchronization error increase while the amplitude ratio change is relatively small. For example, nodes 1 and 2 are almost in phase at 0.1 sec synchronization error in Fig. 6; however, the amplitude ratio is not changed when the input and output are used, or is increased by 2.4% when only output is used. Note that the higher modes are more sensitive to the synchronization error because the phase delay depends on the natural frequency. As shown in Fig. 5 and Fig. 6, the amplitude ratios of the output-only case are affected by the synchronization error, though it is small, which implies the methods using output only are more susceptible to the synchronization error.

The impact of the time synchronization error on the identification of the 2DOF model indicates that the synchronization error distorts significantly the phase information of the estimated modes. However, smart sensors equipped with appropriate hardware and time synchronization protocol have been reported to be synchronized within several milliseconds without significant waste of resources in a system; this level of the synchronization error may be acceptable in many SHM applications.

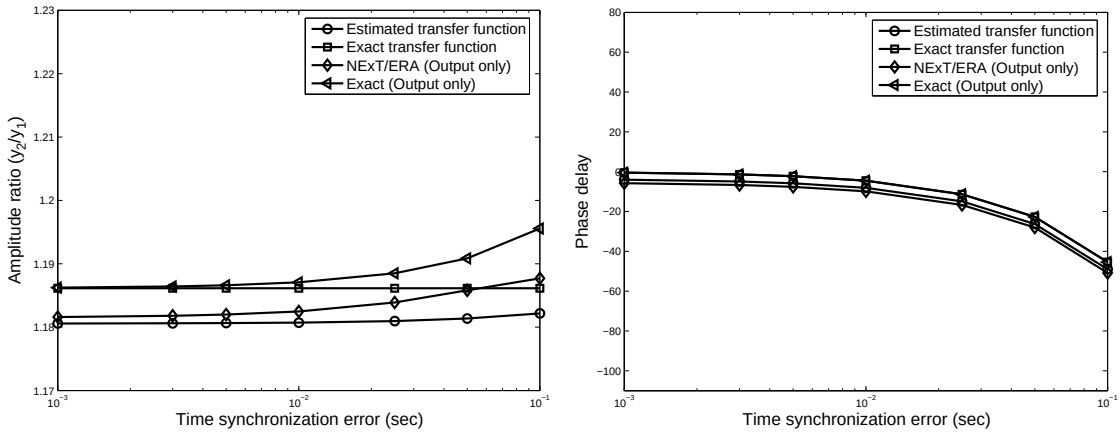

Fig. 5 Comparison between analytical and simulation results in the 1st mode

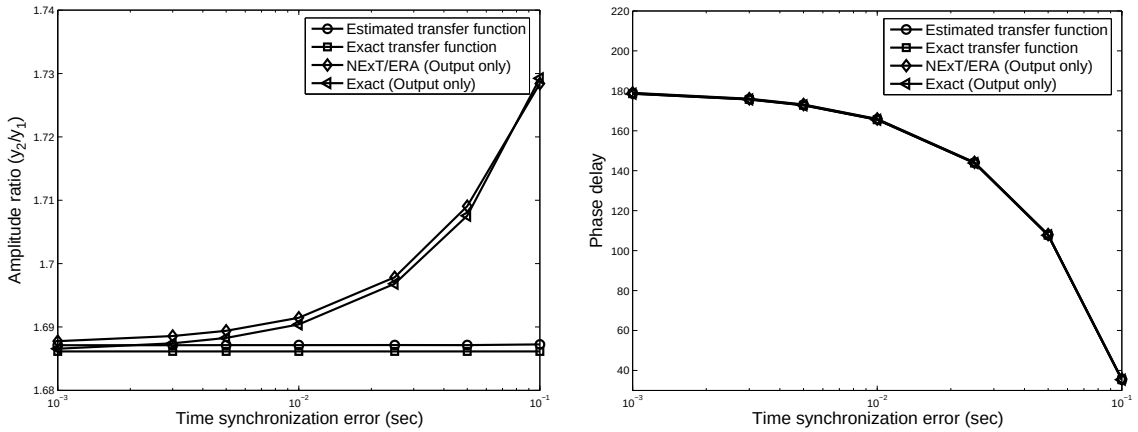

Fig. 6 Comparison between analytical and simulation results in the 2nd mode

4. Effect of Data Loss on SHM

Wireless sensor networks do not necessarily offer reliable data acquisition, which has been assumed in traditional wired SHM systems. Without proper compensation, lost packets can significantly distort the transmitted signals resulting in inaccurate estimates of the modal parameters and false indication of damage status. Reliable communication and proper compensation of lost information are necessary for sound SHM systems. Smart sensors communication protocols can be designed to send acknowledgment messages after receiving data and request to send the lost packets again to have reliable communication. However it is desirable to have simple data transmission without acknowledgement and retransmission when acceptable, because reliably transferring a large amount of vibration measurement data can be challenging. Data transfer allowing data loss is therefore advantageous to save power and avoid network congestion.

In this section, the effect of data loss on PSD estimates is formulated and compared with that of observation noise. Strategies for compensation of the lost data are discussed and their effects on estimation of the PSD, coherence function, and natural frequency are investigated using numerical simulation.

4.1. Compensation approaches

Data loss during wireless communication causes significant errors in subsequent calculations unless appropriately addressed. Measured vibration data in a packet is used to reconstruct a time history on a receiver node. Time stamps or time indeces in a received packet correctly specify where in the reconstructed time history the vibration data in the received packet needs to be expanded. Data loss results in empty space in the reconstructed signal. A way to compensate for the lost data is interpolation using data points around the lost data. “Hold” and “cubic spline” are two major interpolation methods to consider. In the hold method, the previous data is simply used for the lost data. The cubic spline method employs the cubic spline fitting to interpolate the lost data. These two interpolation methods will be considered in an example of SHM procedure and their performance compared.

As well as interpolation methods, the method to construct data packets is considered to have an impact on the subsequent analyses. Since lost information due to packet loss is determined by how packets are constructed, different packetizing methods may result in different accuracy of estimated modal parameters. A simple method of constructing packets, named group packet, is to pack data sequentially, as shown in Fig. 7-(a). When a packet is lost, data loss is concentrated in short time duration. Another method, distributed data packing, in which data in a packet are distributed over the whole data set, is shown in Fig. 7-(b). These two kinds of packets are considered in this section.

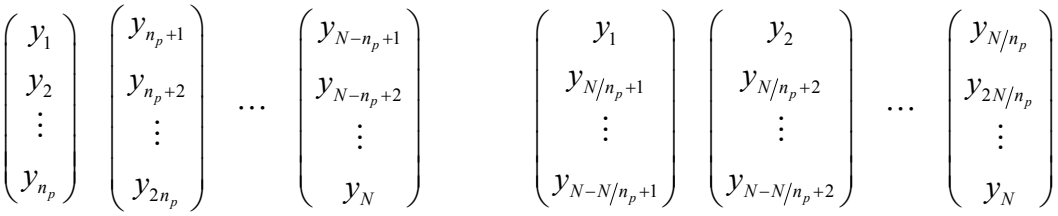

(a) Group packet data (b) Distributed packet data

Fig. 7 Data packet (N : number of data, n_p : number of data in a packet)

4.2. Effect of data loss on PSD and CSD

In this section, PSD of a signal with the distributed packet data loss is investigated to obtain an expression of data loss in terms of equivalent observation noise. The PSD is used in calculating the transfer function from the measured data, which is widely employed in modal analysis using the input and output information. Investigation of data loss on PSD estimation will give an insight into its effect on a SHM systems.

Consider a discrete time sequence $y_n\,(n=1,2,\cdots,N)$. y_n is assumed as a stationary random process. For simplicity, the hold method is used to compensate for the lost data. A total of N_D randomly selected data points are assumed to be lost. Subscript n_{i} ($i=1,2,\cdots,N_D$) corresponds to the lost points. The reconstructed signal in the discrete time domain can be expressed as

$$\overline{y}_n = y_n + \sum_{i=1}^{N_D} A_i \delta_{n-n_i} = y_n + p_n \qquad (n=1,2,\cdots,N) \qquad \text{Eq. (13)}$$

where A_i is the difference between y_n and the interpolated value (i.e., $A_i = y_{n_i-1} - y_{n_i}$), and δ_n is the delta function. p_{n} is discrete time sequence representing difference between y_n and $\overline{y}$. The discrete-time Fourier transform (DFT) of $\overline{y}$ is

given by

$$\bar{Y}_k = \Delta t \sum_{n=0}^{N-1} \bar{y}_n \exp\left[\frac{-j2\pi kn}{N}\right] \qquad \text{Eq. (14)}$$

The PSD of $\bar{y}$ is

$$S_{\bar{y}\bar{y}}(f_k) = \frac{1}{T} E\left[\bar{Y}_k^* \bar{Y}_k\right] = \frac{1}{T}\left[Y_k^* Y_k + P_k^* Y_k + Y_k^* P_k + P_k^* P_k\right] \qquad \text{Eq. (15)}$$

* denotes the complex conjugate. The DFT of p_n is given by

$$P_k = \Delta t \sum_{i=1}^{N_D} A_i \exp\left[\frac{-j2\pi kn_i}{N}\right] \qquad \text{Eq. (16)}$$

The cross spectral density (CSD) between y and p_n can be obtained as

$$S_{p_n y} = \frac{1}{T} E\left[P_k^* Y_k\right] = \frac{1}{T} E\left[\Delta t^2 \sum_{n=1}^{N}\sum_{i=1}^{N_D} y_n A_i \exp\left[\frac{-j2\pi k(n-n_i)}{N}\right]\right] \qquad \text{Eq. (17)}$$

By taking the expectation of $y_n A_i$ first,

$$\begin{aligned} S_{p_n y} &= \frac{\Delta t}{N}\sum_{n=1}^{N}\sum_{i=1}^{N_D}\left(R\left(\left(n-n_i+1\right)\Delta t\right) - R\left(\left(n-n_i\right)\Delta t\right)\right)\exp\left[\frac{-j2\pi k(n-n_i)}{N}\right] \\ &\cong \frac{N_D}{N}\Delta t \sum_{l=-(N-1)}^{N-1}\left(R\left(\left(l+1\right)\Delta t\right) - R\left(l\Delta t\right)\right)\left(1-\frac{|l|}{N}\right)\exp\left[\frac{-j2\pi kl}{N}\right] \qquad \text{Eq. (18)} \\ &\cong \frac{N_D}{N}\left(\exp\left[\frac{j2\pi k}{N}\right]-1\right)S_{yy} \end{aligned}$$

where $R(t)$ is the autocorrelation function of y_n. Using Eq. (16) and assuming that $E\left[A_i A_j\right]$ $(i \neq j)$ is negligible due to the assumption that the lost points are sparse,

$$
\begin{aligned}
S_{pp}(f_k) &= \frac{1}{T} E\left[P_k^* P_k \right] \\
&= \frac{\Delta t^2}{T} \sum_{i=1}^{N_D} E\left[A_i^2 \right] \\
&= \frac{2\Delta t \cdot N_D}{N} \left(R(0) - R(\Delta t) \right)
\end{aligned}
\qquad \text{Eq. (19)}
$$

where Δt is the time step. From Eq. (15), Eq. (18), and Eq. (19), the error in the PSD estimation defined by $\varepsilon\left[S_{yy} \right] = S_{\overline{yy}} - S_{yy}$ is

$$
\varepsilon\left[S_{yy} \right] \cong \frac{2N_D}{N} \left(\cos\left(\frac{2\pi k}{N} \right) - 1 \right) S_{yy}(f_k) + \frac{2\Delta t \cdot N_D}{N} \left(R(0) - R(\Delta t) \right) \qquad \text{Eq. (20)}
$$

The first term in the right side of Eq. (20) is proportional to S_{yy} and much smaller than S_{yy} due to N_D / N. However, the second term is constant over frequency. This term can be large compared to S_{yy} at zeros of a system; indeed, S_{yy} is extremely small at zeros of a system. The overall shape of the PSD is therefore mainly determined by the second term.

In contrast to the PSD, the CSD is less susceptible to either data loss or measurement noise. Since correlation between the data loss terms p_n of two different signals is small, the cross spectrum of the two data loss can be assumed zero (i.e., $S_{p_1 p_2} = 0$). Thus, CSD is only affected by the cross terms between the signal and data loss, which do not significantly blur zeros of the system. The output-only modal analysis utilizes CSD mostly and a limited number of PSD at reference points; the input-output modal analysis requires PSD to obtain each transfer function. The output-only modal analysis is therefore expected to outperform the methods using both of input and output with respect to data loss.

Comparison of the second term with the error in the PSD estimation induced by the observation noise reveals the data loss level in terms of the noise level. Consider the white noise with the standard deviation σ_n. The PSD of the noise is constant in the frequency domain and represented as $\sigma_n^2 \cdot \Delta t$. An equation to relate the observation noise level with the data loss level in Eq. (19) can be written as follows.

$$\frac{2\Delta t \cdot N_D}{N}\left(R(0) - R(\Delta t)\right) = \sigma_n^2 \cdot \Delta t \qquad \text{Eq. (21)}$$

Let the RMS noise level and the data loss level be ρ_n and ρ_d, respectively.

$$\rho_n = \frac{\sigma_n}{\sigma_y}$$
$$\rho_n = \frac{\#\text{ of lost data}}{\#\text{ of data}} \qquad \text{Eq. (22)}$$

where σ_y is the standard deviation of y_n. Eq. (21) is then simplified as

$$\rho_d = \frac{\rho_n^2}{2\left(1 - \frac{R(\Delta t)}{R(0)}\right)} \qquad \text{Eq. (23)}$$

Data loss is shown to have similar effect on PSD as observation noise. Though not derived analytically here, Eq. (23) is expected to hold for subsequent analyses, i.e., modal analysis and damage detection. This conjecture, as well as the effect of packetizing, is investigated with numerical simulation.

4.3. Example

A computer simulation is conducted for a truss model to investigate the effects of data loss on the procedure of the SHM. The selected model is a 53DOF statically determinate

structure as shown in Fig. 8. Each element has a Young's modulus of 200GPa and cross-sectional area of 112.2m^2. The truss is vertically excited at node 6 with the band-limited white noise, and the vertical accelerations of the bottom nodes (node 2~14) are measured. After data is acquired at the sampling frequency of 380 Hz, a certain percentage of packets are randomly dropped to simulate data loss. Two ways of data loss, group and distributed packet data, are applied to the simulated acceleration of the planar truss model. In this simulation, the size of packet is selected to be 8. The lost points are selected randomly, and the hold and cubic spline methods are used to interpolate lost data. ERA is employed in modal analysis. Each simulation is repeated 100 times and averaged. The simulation results are shown in Fig. 11 and Fig. 12.

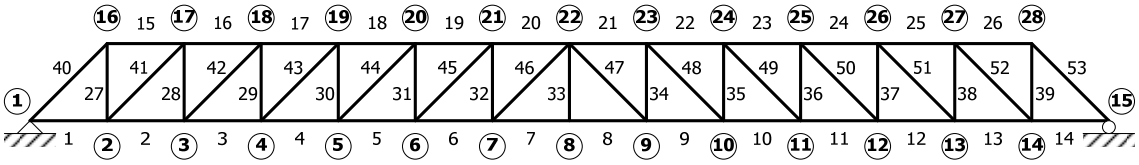

Fig. 8 Planar truss model

To verify Eq. (23), the outcome is compared to that of the computer simulation including observation noise (but without data loss). A band-limited white noise is added to each of the observed signals. The RMS noise level is specified as a percentage of the RMS of physical response. Data loss level of 0.38% is estimated from Eq. (23) to have similar effects on power spectral density as observation noise of 5%. Fig. 9 shows both of data loss and noise result in the same effect on the PSD and coherence function.

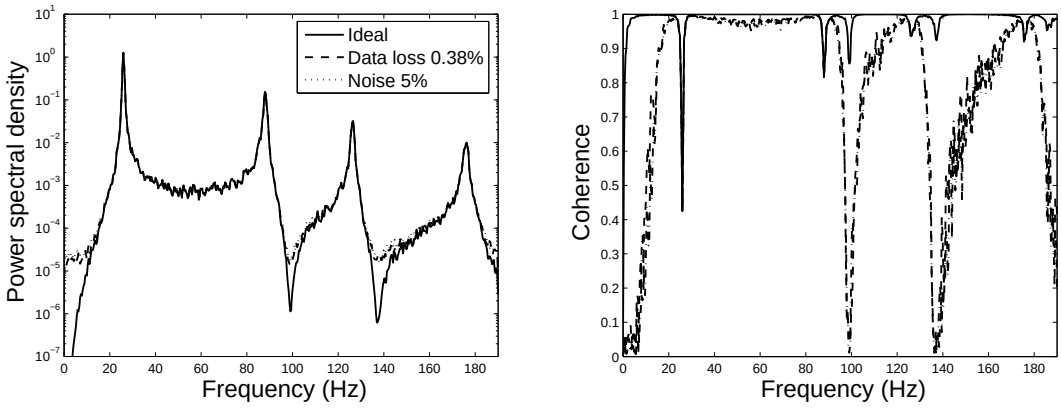

Fig. 9 Data loss effect on power spectral density and coherence at node 10

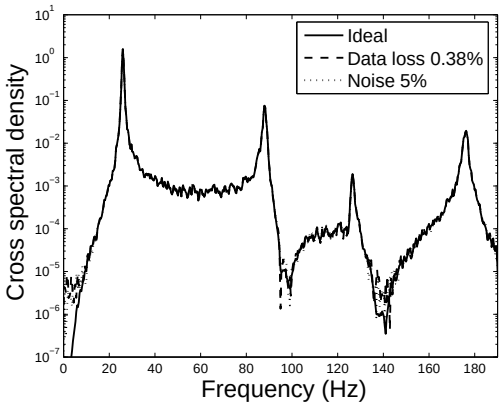

Fig. 10 Data loss effect on cross spectral density between node 8 and 10

The loss of data reduces the coherence function except at the system's poles (see Fig. 9). Because of the random nature of data loss occurrence and the excitation, the coherence function varies from simulation to simulation. In FFT calculations, twenty averages are used. The coherence function's deviation from unity depends on the input and output, between which the function is calculated. All the investigated coherence function plots, however, support 10 % noise addition affects the coherence function in a similar way as the loss of 0.5~ 2.5 % data does, which agrees with what Eq. (23) suggests for PSD.

The zeros of the estimated CSDs of accelerations at node 8 and 10 remain clear

with either data loss or measurement noise (See Fig. 10). Although there is some difference at the zeros, both data loss and measurement noise do not distort the CSD significantly as compared to the PSD plot in Fig. 9. Randomness of data loss and noise makes $S_{p_1 p_2} = 0$, resulting in an accurate estimation of the CSD. Note that the two CSDs with data loss and measurement noise are close to each other, which implies Eq. (23) still hold for CSD estimation and modal analysis using output only.

Fig. 11 and Fig. 12 illustrate the errors in the estimated natural frequencies under the various levels of data loss. The errors are calculated with respect to the estimated natural frequencies without any data loss. These figures reveal the cubic spline method does not give a significant benefit in spite of the additional computation required. When the hold method is used, both of the group and distributed packets provide a similar level of accuracy overall. However, the effect of these two packetizing methods on the damage detection algorithm employed in a SHM system should be investigated before selecting one of them. In addition, the modal analysis methods using only output information are found more robust against both of data loss and noise by comparing Fig. 11 and Fig. 12. The mean and standard deviation of the error are significantly reduced in Fig. 12, which agrees with the small errors in estimation of CSD with data loss and noise.

The relationship between noise and data loss, Eq. (23), can be verified to hold for modal analysis in Fig. 11 and Fig. 12. The distributed packet and hold method are assumed when Eq. (23) is obtained in the previous section. The estimated natural frequencies from the distributed packet and hold methods exhibit close error mean and standard deviation to those of the noise case in Fig. 11 and Fig. 12. The mean error

in Fig. 12 are difficult to distinguish; however, if zoomed in, they are close. Particularly Fig. 12 indicates that Eq. (23) works for the methods using output only as expected from CSD estimation.

In this example, the effect of data loss on the SHM system is discussed. The PSD estimates from the simulated data validate Eq. (23), the relationship between data loss and observation noise level. Even though not verified analytically, Eq. (23) appears to hold for other function estimates and the subsequent analysis results, such as CSD, coherence, and the natural frequency estimation. The hold method with either group or distributed packet is recommended in a SHM system allowing small amounts of data loss.

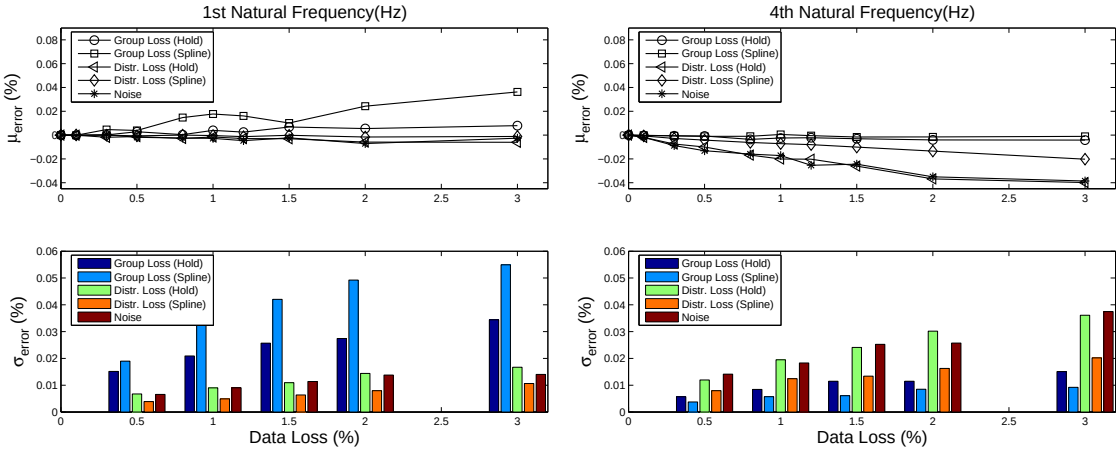

Fig. 11 Errors of estimated natural frequencies when input and output are used

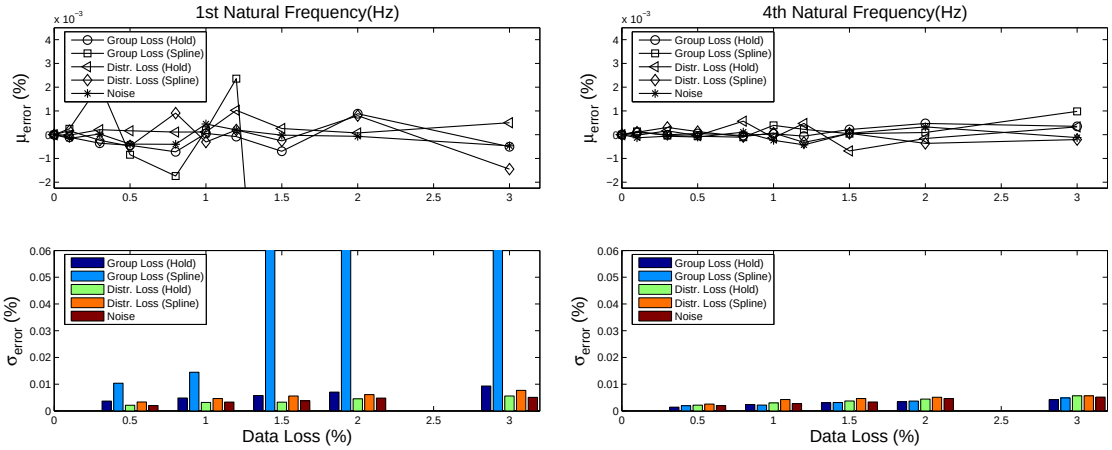

Fig. 12 Errors of estimated natural frequencies when only output is used

5. COORDINATED COMPUTING

The amount of data involved in SHM applications normally exceeds practical communication capabilities of smart sensor networks if all the measurement data needs to be collected centrally; data aggregation has been an important issue to be addressed before a SHM system employing smart sensors is realized. One approach to overcome this data aggregation problem has been an independent data processing strategy. This approach, however, cannot fully exploit information available in the sensor network. Distribution of data processing and coordination among smart sensors play central roles in addressing many smart sensor implementation issues, including data aggregation. This section will demonstrate that distribution and coordination can be well planned so that the data aggregation problem is addressed without sacrificing structural analysis performance. Two examples of distributed computing based on SHM analyses are provided to illustrate the approach.

5.1. Distributed implementation of correlation function estimation

Correlation function estimation is oftentimes the beginning step of output-only SHM of

civil infrastructure and usually involves a large amount of measurement data (Gao 2005). Cross-correlation estimation needs data from two sensor nodes. Measured data needs to be transmitted from one node to the other before the processing takes place. Associated data communication can be prohibitively large without careful consideration for implementation. Distribution of data processing and coordination among smart sensors are addressed herein to incorporate application specific knowledge into data aggregation.

Correlation functions are, in practice, estimated from finite length records. Power and cross spectral density (PSD/CSD) functions are estimated first through the following relation (Bendat and Piersol 2000):

$$G_{xy}(\omega) = \frac{1}{n_d T} \sum_{i=1}^{n_d} X_i^*(\omega) Y_i(\omega) \qquad \text{Eq. (24)}$$

where $G_{xy}(\omega)$ is CSD estimation between two stationary Gaussian random process, $x(t)$ and $y(t)$. $X(\omega)$ and $Y(\omega)$ are the Fourier transform of $x(t)$ and $y(t)$; the * denotes the complex conjugate. T is time length of sample records, $x_i(t)$ and $y_i(t)$. When $n_d = 1$, the estimate has a large random error. The random error is reduced by computing an ensemble of the estimates from n_d different or partially overlapped records. The normalized RMS error $\varepsilon\left[\left|G_{xy}(\omega)\right|\right]$ of the spectral density function estimation is given as

$$\varepsilon\left[\left|G_{xy}(\omega)\right|\right] = \frac{1}{\left|\gamma_{xy}\right|\sqrt{n_d}} \qquad \text{Eq. (25)}$$

γ_{xy} is the coherence function between $x(t)$ and $y(t)$, indicating the degree of

linearity between them. Through the averaging process, the estimation error is reduced. Averaging of 10-20 times is common practice. The estimated spectral densities are then converted to correlation functions by inverse Fourier transform.

An implementation of correlation function estimation for a small community of sensors in a centralized data collection scheme is shown in Fig. 13. where node 1 works as a reference sensor. Assuming n_s nodes, including the reference node, are measuring structural response, each node acquires data and sends to the reference node. The reference node calculates the spectral density as in Eq. (24). This procedure is repeated n_d times and averaged. After averaging, the inverse FFT is taken to calculate the correlation function. All the calculation takes place at the reference nodes. When the spectral density is estimated from discrete time history records of length N, data to be transmitted through the radio is $N \times n_d \times (n_s - 1)$.

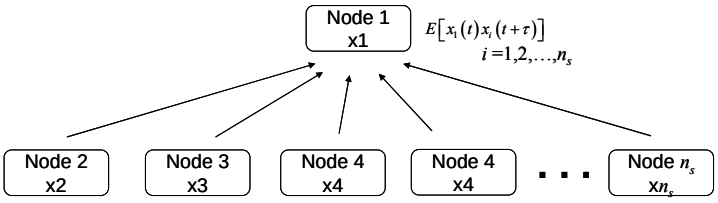

Fig. 13 Centralized NExT implementation

In the next scheme, data flow for correlation function estimation is examined and data transfer is reorganized to take advantage of computational capability on each smart sensor node. After the first measurement, the reference node broadcasts the time record to all the nodes. On receiving the record, each node calculates the spectral density between its own data and the received record. This spectral density estimate is locally stored. The nodes repeat this procedure n_d times. After each measurement, the stored

value is updated by taking a weighted average between the stored value and the current estimate. In this way, Eq. (24) is calculated on each node. Finally the inverse FFT is applied to the spectral density estimate locally. The resultant correlation function is sent back to the reference node. Because the subsequent modal analysis such as ERA uses, at most, half of the correlation function data length, $N/2$ data is sent back to the reference node from each node. The total data to be transmitted in this scheme is, therefore, $N \times n_d + N/2 \times (n_s - 1)$ (see Fig. 14).

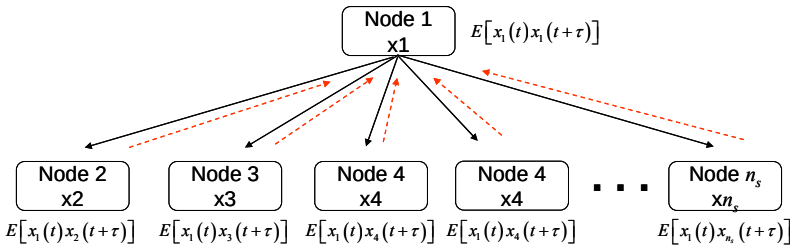

Fig. 14 Distributed NExT implementation

As the number of nodes increases, the advantage of the second scheme, in terms of communication requirements, becomes significant. The second approach requires data transfer of $O\left(N \cdot \left(n_d + n_s\right)\right)$, while the first one needs to transmit to the reference sensor node data of the size of $O\left(N \cdot n_d \cdot n_s\right)$. The distributed implementation leverages knowledge regarding the application to reduce communication requirements as well as to utilize CPU and memory in a smart sensor network efficiently.

The data communication analysis above assumes that all the nodes are in single-hop range of the reference node. This assumption is not necessarily the case for a general SHM application. However, Gao (2005) proposed a Distributed Computing Strategy (DCS) for SHM which support this idea. Neighboring smart sensors in a

single-hop communication range make local sensor communities and perform SHM in the communities. In such applications, the assumption of nodes being in single hop range of a reference node is reasonable.

5.2. Distributed Computing Strategy (DCS)

The DCS for SHM proposed by Gao (2005) is suitable for implementation on networks of densely distributed smart sensors. The conceptual hierarchical organization of the DCS approach is shown in Fig. 15. In contrast to traditional SHM algorithms which require all the measured information to be transferred to a central station, the measured information is aggregated locally by a selected sensor within the sensor group, termed the manager sensor, and only limited information is sent back to the central station to provide the condition of the structure. Small numbers of smart sensors are grouped to form different communities so that all sensors in a community are located in the range of single hop. Although each sensor in Fig. 15 is included in only one community, in the DCS approach smart sensors can be contained in multiple communities. Each manager sensor collects necessary information and implements the damage detection algorithm for its community. Adjacent manager sensors interact with each other to exchange information. In Fig. 15, manager sensors in communities 1, 2, and 3 interact with each other while community 4 does only with community 3. Once information is aggregated, the manager sensors determine information to be sent back to the central station. The manager sensor of the community in which damage has not occurred transmits only an "OK" signal to the central station. If damage has occurred, the manager sensor of the community needs to send damage information such as damage location, which is reflected by the solid line in Fig. 15. Thus, the DCS approach requires only limited

information need to be transferred between sensors throughout the entire sensor network. This approach will significantly reduce the communication traffic in the sensor network.

Gao (2005) shows that NExT (James et al. 1992), Eigensystem Realization Algorithm (Juang and Pappa 1985), and Damage Locating Vector method (Bernal 2002) can be utilized as structural analysis techniques to materialize this DCS concept. These structural analyses are applied in each sensor community. The manager sensors communicate with each other to assess mode shapes' normalization constants and to make redundant judgment about damaged element; most of data processing and communication takes place inside each sensor community. Coordination among smart sensors employing DCS, which has yet to be implemented, is expected to realize a SHM system using densely installed smart sensors.

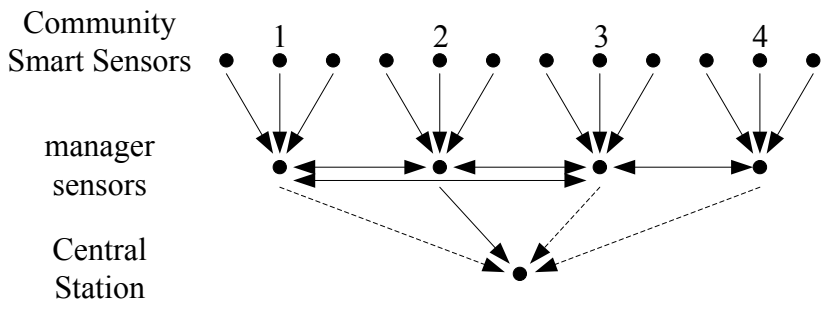

Fig. 15 Sketch of hierarchical organization

5.3. Implementation on smart sensors

In this section, distributed computing is implemented on a network of smart sensors. The distributed implementation of correlation function estimation is incorporated into DCS; correlation function estimation in DCS is conducted in the distributed manner. Then ERA is applied at a manager sensor to estimate modal parameters. The rest of

DCS, i.e, DLV and communication between manager sensors, is currently being implemented. SHM performance is examined in terms of accuracy of signal processing, while data aggregation performance is assessed from reduction in communication requirements during correlation function estimation.

The smart sensor platform used in this demonstration is Imote2. Imote2 has Intel Xscale processor and 256KB of RAM. Radio components has data rate of 250 Kbps. 256KB of RAM on Imote2 allows implementation of correlation function estimation from a large amount of data and ERA involving large Hankel and system matrices. An open source operating system, TinyOS, is utilized to program Imote2s. The hardware is appropriate for data processing intensive applications such as SHM

To understand the performance of the algorithms, the coordinated computing implemented on Imote2 is demonstrated using a numerical truss model shown in Fig. 8. Vertical acceleration responses under random input are measured at nodes 5 to 13 and injected into a network of nine Imote2s. The Imote2 corresponding to node 5 works as the reference sensor. This node broadcast its own data to the other node and collect correlation function estimate. Once all the correlation function estimates are collected, this reference node applies ERA to obtain natural frequencies, damping ratios and mode shapes. The length, N, of the injected data is 2048 and the number of FFT points is 512, resulting in 7 times averaging with 50 % overlap. The sampling rate is 500 Hz.

The acceleration response data and correlation function estimates are stored and transferred in 16-bit integer data type, considering that accelerometer's resolution can be reasonably assumed to be around 12-bit. In this way, memory space and bandwidth are efficiently utilized, though cast double precision data is used during

NExT and ERA.

Although a certain amount of data loss is shown to be acceptable in the previous section, reliable communication is used in this demonstration. In this way, outputs of this coordinated computing, i.e., correlation function estimates, natural frequencies, damping ratios, and mode shapes, are compared with those calculated on a PC without mixing with the effect of data loss.

Correlation functions are first estimated on the Imote2s and reported back to the reference node. Fig. 16 shows the estimated correlation function between node 5 and node 6. This estimate matches the corresponding correlation function estimated on a PC assuming associated quantization error. Because the difference between these two signals is smaller than 10^{-13}, only the estimate on a Imote2 is shown on Fig. 16.

Correlation function estimates collected at the reference sensor node are then analyzed with ERA. TABLE 3 summarizes the identified modal parameters. Natural frequencies and damping ratios are compared with those determined on a PC. Modal assurance criteria (cite a reference) are utilized to compare mode shapes. All of the identified parameters are consistent with calculation on a PC. Together with the correlation function estimates, this result demonstrates that this coordinated computing approach can perform SHM analysis accurately.

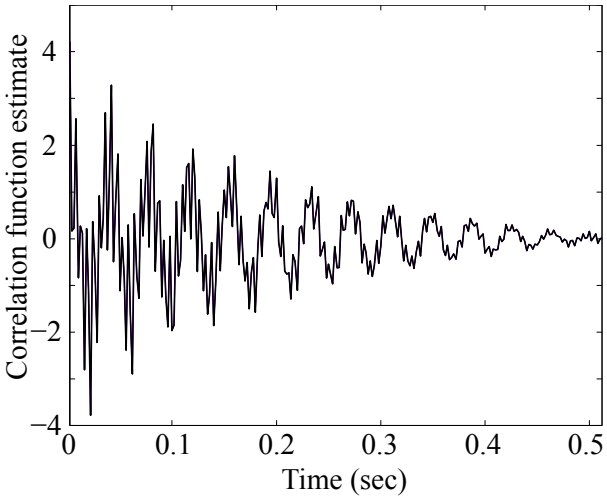

Fig. 16 A correlation function estimate

Table 3 Results of modal analysis performed on Imote2

Mode	*1*	*2*	*3*	*4*
Natural Frequency (Hz)	27.21	97.23	127.36	176.14
Error(ratio)	-2.13E-13	3.26E-13	-3.20E-13	1.71E-13
Damping ratio (%)	4.09	10.35	5.32	0.43
Error (ratio)	-2.93E-14	1.08E-13	-1.31E-13	1.02E-14
Modal Assurance Criteria of mode shapes - 1	0	-2.22E-16	-2.22E-16	0

Data transferred in a network is reduced as explained in 6.1. In this example, data transmission is reduced by a factor of 5, as compared to centralized NExT implementation. This reduction factor can be larger depending on the number of sensors and the associated averaging. This reduction shows the advantage of distributed correlation function estimation.

Further consideration is necessary to accurately assess the efficacy of the distributed implementation. Power consumption of smart sensor networks is not simply proportional to the amount of data transmitted. Acknowledgement messages and synchronization messages are also involved. The radio listening mode consumes power even when no data is received. However, the size of the measured data is usually much larger than the size of the other messages to be sent and should be considered the

primary factor in determining power consumption. Small data transfer requirements will lead to small power consumption.

6. CONCLUSION

Although smart sensor usage in SHM applications is promising, full-fledged SHM systems employing smart sensors have not yet been realized. Critical issues such as time synchronization error, data loss, and a large amount of data have been described and investigated.

Time synchronization error was formulated and its effects on SHM applications investigated. Input-output identification and output-only identification were reviewed with time synchronization error taken into account. Mode shape phase was shown to be sensitive to time synchronization error. The impact is not negligible when the ratio of time synchronization error to a natural frequency of a system is large. However, time synchronization accuracy reasonably available for smart sensors and low natural frequencies of a large structure oftentimes result in small impact on modal analysis.

Data loss was investigated with respect to the performance of the modal parameter estimation. An expression was derived relating the amount of data loss to an equivalent measurement noise. Two types of packet arrangement were considered and shown to have a similar level of accuracy in most cases. Data loss is found to introduce error into the modal analysis, which also affects the subsequent analysis. Because of the averaging associated with the PSD and the CSD estimation, a certain amount of data loss can be accommodated. Particularly, the CSD estimation is found to be robust against both of data loss and observation noise, allowing the output-only identification to be better than the one using input and output.

Coordinated computing is shown to be an effective approach for SHM applications, especially for data aggregation. Two examples of coordinated computing supported by structural analysis are shown. Implementation on Imote2s demonstrates the efficacy of this approach.

ACKNOWLEDGEMENTS

This study is supported in part by the National Science Foundation under grant CMS 0301140 (Dr. S. C. Liu, program manager). Partial support from Vodafone, Korea Science and Engineering Foundation, Kitami Institute of Technology, and Japan Ministry of Education, Culture, Sports, and Technology is gratefully appreciated. The support is gratefully acknowledged.

REFERENCES

Arici, Y. and Mosalam, K. M., 2003, "Modal Analysis of a Densely Instrumented Building Using Strong Motion Data", *Proceedings of the International Conference on Applications of Statistics and Probability in Civil Engineering*, San Francisco, CA, June 6-9, 419-426.

Bendat, J. S. and Piersol, A. G. (2000), *Random data: analysis and measurement procedures*, John Wiley and Sons, Inc. New York, NY.

Bernal, D. (2000), "Extracting flexibility matrices from state-space realization.", *COST F3 Conf.,* Madrid, Spain, 127-135.

Bernal, D. (2002), "Load vectors for damage localization", *Journal of Engrg. Mech.*, 128(1):7-14.

Casciati, F., Faraveli, L. and Borghetti, F., 2003, "Wireless Links between

Sensor-Device Control Stations in Long Span Bridges", Smart Structures and Materials 2003: Smart Systems and Nondestructive Evaluation for Civil Infrastructures, *Proceedings of the SPIE*, Vol. 5057, San Diego, CA, pp. 1-7

Celebi, M. (2002), "Seismic instrumentation of buildings (with emphasis on federal buildings)" *Special GSA/USGS Project, an administrative report*, United States Geological Survey, Menlo Park, CA.

Crossbow Technology, Inc. http://www.xbow.com

Doebling, S. W., Farrar, C. R., Prime, M. B., and Shevitz, D. W. (1996), "Damage identification and health monitoring of structural and mechanical systems from changes in their vibration characteristics: a literature review", *LA-13070-MS*.

Doebling, S. W., Farrar, C. R., and Prime, M. B. (1998), "A summary review of vibration-based damage identification methods", *The Shock and Vibration Digest*, vol. 30, no. 2, pp. 91-105.

Doebling, S. W. and Farrar, C. R. (1999), "The state of the art in structural identification of constructed facilities", *A report by American Society of Civil Engineers Committee on Structural Identification of Constructed Facilities*.

Elson, J., Girod, L. and Estrin, D. (2002), "Fine-Grained Network Time Synchronization using Reference Broadcasts", Proc. of the Fifth Symposium on Operating Systems Design and Implementation (OSDI 2002).

Farrar, C. R. (2001), "Historical overview of structural health monitoring", *Lecture Notes on Structural Health Monitoring using Statistical Pattern Recognition*, Los Alamos Dynamics, Los Alamos, NM.

Gao., Y. (2005), “Structural health monitoring strategies for smart sensor networks.” PhD Dissertation, University of Illinois at Urbana-Champaign.

Gros, X. E. (1997), *NDT data fusion*, Arnold, London, UK.

Hollar, S. (2000), COTS Dust., Master's Thesis, University of California, Berkeley, CA.

James, G. H., Carne, T. G., and Lauffer, J. P. (1993), “The natural excitation technique for modal parameter extraction from operating wind turbine”, *Report No. SAND92-1666, UC-261*, Sandia National Laboratories, Sandia, NM..

James, G. H., Carne, T. G., Lauffer, J. P., and Nord, A. R. (1992), “Modal testing using natural excitation”, *Proceedings of 10th Int. Modal Analysis Conference*, San Diego, CA.

Kottapalli, V. A., Kiremidjian, A. S., Lynch, J. P., Carryer, E., Kenny, T. W., Law, K. H., and Lei, Y., 2003, “Two-tiered Wireless Sensor Network Architecture for Structural Health Monitoring”, in Smart Structures and Materials, San Diego, CA, March 3-6, *Proceedings of the SPIE*, Vol. 5057, 8-19.

Kurata, N., Spencer, B. F. Jr., and Ruiz-Sandoval, M., 2004, “Building Risk Monitoring Using Wireless Sensor Network”, *Proceedings of the 13th World Conference on Earthquake Engineering*, August 2-6, Vancouver, BC, Cananda.

Lei, Y., Kiremidjian, S., Nair, K.K., Lynch, J.P. and Law, K.H. (2004), “Algorithms for time synchronization of wireless structural monitoring sensors”, *Earthquake Engng Struct. Dyn.*, 34:555-573.

Lyncn, J. P., Wang, Y., Law, K. H., Yi, J.-H., Lee, C. G., Yun, C. B. (2005), “Validation of a large-scale wireless structural monitoring system on the Geumdang bridge.”, *Proceedings of the Int. Conference on Safety and Structural Reliability*, Rome, Italy

Lynch, J. P. and Loh, K. J. (2006), "A summary review of wireless sensors and sensor networks for structural health monitoring", *Shock and Vibration Digest*, 38(2), 91-128.

Mechitov, K., Kim, W., Agha, G., and Nagayama, T. (2004), "High-frequency distributed sensing for structure monitoring", *Proceedings of 1st Int. Workshop on Networked Sensing Systems*, 101-105

Nagayama, T., Ruiz-Sandoval, M., Spencer Jr., B. F., Mechitov, K. A., Agha, G.. A. (2004), "Wireless strain sensor development for civil infrastructure", *Proceedings of 1st Int. Workshop on Networked Sensing Systems*, Tokyo, Japan, 97-100.

Nagayama, T., Abe, M., Fujino, Y. And Ikeda, K. (2005), "Structural Identification of a Nonproportionally Damped System and Its Application to a Full-Scale Suspension Bridge", *Journal of Structural Engineering*, Vol. 131, No. 10, 1536-1545.

Nagayama, T., Spencer, Jr., B. F., Agha, G. A., and Mechitov, K. A. (2006), "Model-based data aggregation for structural monitoring employing smart sensors", *Proceedings of the Third International Conference on Networked Sensing Systems (INSS 2006)*, May 31- Jun 2, pp. 203-210.

Nitta, Y., Nagayama, T., Spencer Jr., B. F., and Nishitani, A. (2005), "Rapid damage assessment for the structures utilizing smart sensor MICA2 MOTE", *Proceedings of 5th Int. Workshop on Structural Health Monitoring*, Stanford, CA., 283-290

Salawu, O. S. and Williams, C. (1995), "Review of full-scale dynamic testing of bridge structures", *Engineering Structures*, vol. 17, no. 2, pp. 113-121.

Sohn, H., Farrar, C. R., Hemez, F. M., Shunk, D. D., Stinemates, D. W., and Nadler, B. R. (2001), "A review of structural health monitoring literature: 1996-2001", *Los Alamos*

National Laboratory Report, LA-13976-MS.

Spencer Jr., B. F., Ruiz-Sandval, M. E. and Kurata, N. (2004), "Smart sensing technology: opportunities and challenges", Structural Control and Health Monitoring, 11:349-368.

Ruiz-Sandoval, M. (2004), "Smart sensors for civil infrastructure systems", Ph.D. Dissertation, University of Notre Dame, IN.

Ruiz-Sandoval, M., Nagayama, T., and Spencer, B.F. (2006), "Sensor development using Berkeley Mote platform", *Journal of Earthquake Engineering*, 10(2), 289-309.

Wang, Y., Lynch, J. P., and Law, K. H. (2005), "Wireless Structural Sensors Using Reliable Communication Protocols for Data Acquisition and Interrogation", *Proceedings of the 23rd International Modal Analysis Conference (IMAC XXIII)*, Orlando, FL, January 31-February 3.

Wong, K. Y. (2004), "Instrumentation and health monitoring of cable-supported bridges", *Structural Control and Health Monitoring*, 11(2), 91-124